

Article

A Comparative Study of Polypyrrole and Ag/Polypyrrole Hybrid Nanocomposites as Sensitive Material Used for New Dry Polarizable Bioimpedance Sensors

Gabriela Telipan, Lucian Pîslaru-Dănescu * , Eduard-Marius Lungulescu , Ioana Ion and Virgil Marinescu

National Institute for Research and Development in Electrical Engineering ICPE-CA, 313, Splaiul Unirii, 030138 Bucharest, Romania; gabriela.telipan@icpe-ca.ro (G.T.); marius.lungulescu@icpe-ca.ro (E.-M.L.); ion.ioana@icpe-ca.ro (I.I.); virgil.marinescu@icpe-ca.ro (V.M.)

* Correspondence: lucian.pislaru@icpe-ca.ro

Featured Application: Authors are encouraged to provide a concise description of the specific application or a potential application of the work. This section is not mandatory.

Abstract: Three types of dry polarizable electric bioimpedance sensor for skin bioimpedance monitoring without skin preparation have been developed. The sensitive materials as a component of these sensors are the conductive polypyrrole and hybrid nanocomposite polypyrrole-Ag, with 10% and 20% Ag incorporated in the polypyrrole matrix. The hybrid nanocomposites Ag nanoparticles (NPs)/polypyrrole were obtained by introducing the colloid solution of Ag NPs in pyrrole solution, followed by polymerisation, and calculated for 10% and 20% of monomer's mass. The structural characterisation and morphological analysis of these sensitive materials were carried-out by Raman spectrometry, Fourier transform infrared (FTIR) spectroscopy, scanning electron microscopy, and energy-dispersive X-ray spectroscopy. In making the electrodes, the technique of pressing powders of polypyrrole and hybrid composites Ag NPs/polypyrrole in a hydraulic press was used in the form of a disk. The electric bioimpedance performance of sensors was investigated using a two-point method in the frequency range of 1–300 kHz, at a voltage of $2 V_{\text{peak-peak}}$, on six human subjects, three men and three women. For these three bioimpedance sensors, it was found that the electric bioimpedance of the skin decreases across the frequency range and shows good linearity of the impedance-frequency curve on the range frequency of interest in bioimpedance measurements.

Keywords: polypyrrole; hybrid nanocomposite Ag/polypyrrole; dry polarizable bioimpedance sensor; electric bioimpedance



Citation: Telipan, G.; Pîslaru-Dănescu, L.; Lungulescu, E.-M.; Ion, I.; Marinescu, V. A Comparative Study of Polypyrrole and Ag/Polypyrrole Hybrid Nanocomposites as Sensitive Material Used for New Dry Polarizable Bioimpedance Sensors. *Appl. Sci.* **2021**, *11*, 4168. <https://doi.org/10.3390/app11094168>

Academic Editor:

Joamin Gonzalez-Gutierrez

Received: 22 March 2021

Accepted: 29 April 2021

Published: 2 May 2021

Publisher's Note: MDPI stays neutral with regard to jurisdictional claims in published maps and institutional affiliations.



Copyright: © 2021 by the authors. Licensee MDPI, Basel, Switzerland. This article is an open access article distributed under the terms and conditions of the Creative Commons Attribution (CC BY) license (<https://creativecommons.org/licenses/by/4.0/>).

1. Introduction

Electrical impedance of biological tissue, named electric bioimpedance, is used for medical diagnosis due to properties such as the possibility of monitoring organs and tissues' state, both in vivo and in vitro modes. Moreover, it can offer the relatively simple possibility of technological achievement for bioimpedance sensors [1]. Bioimpedance presents an advantage because it is a technique that provides health information in a non-invasive way. This medical technique involves an injection of alternating electric current in human tissues at very low intensity. In the technique of bioimpedance measurements, performed under the influence of the injected electric current, the biologic tissues, organs, cells medium behave like conductors, dielectrics, or insulators, each depending on their composition. Because of this phenomenon, bioimpedance dependence on frequency produces much information about the biological medium's psychological state under investigation [2]. This investigation refers to the changes taking place in organs, muscle, nerves, brain, heart, skin, eye retina in establishing a diagnosis, can be made by clinical methods, like ECG

(electrocardiogram), EMG (electromyogram), EOG (electrooculogram), ESR (galvanic skin reflex), electrooculography, electroencephalography (EEG) [3–9].

Bioimpedance sensors must meet several requirements, such as being non-invasive, portable, user-friendly, and low cost [2]. A skin inclusive ECG electrode is a contact sensor that produces an electrical interface between the body and the measurement system, allowing the electrical charges to flow through the tissue and sense endogenous biopotential [10].

The bioimpedance electrodes are classified into polarizable and non-polarizable electrodes, also known as dry or wet electrodes. In the case of a polarizable electrode, no electrode reactions occur when an electrical potential is applied, and no charge flows across the electrode–electrolyte interface. In this case, the electrode behaves as a capacitor. In the case of non-polarizable electrode, the electrode will not change from its equilibrium potential in the presence of a density of electric current, which appeared due to the injection of a constant current. For this type of electrode, the current flows freely across the electrode without producing any electric potential. An ideal non-polarizable electrode exhibits a resistive behaviour, with a nominal resistance value that is ideally zero [10,11]. The polarizable electrodes are more suitable for sensing biopotentials, while non-polarizable electrodes are more suitable for current stimulation by current injection [12].

Ag/AgCl is the most common non-polarizable wet electrode and requires a gel electrolyte to work properly. The use of the gel leads to many negative effects over time, such as: it reduces the resistance between the surface of the metal part of the electrode and the skin below the stratum corneum (SC) layer; it increases the dielectric constant between skin and electrode, and operates for short time because of degradation of conductivity as the electrode interface and the impedance changes over time, from gel evaporation, so, the signal quality of the electrodes decreases. The long-term contact between the gel and the skin can also produce unwanted adverse reactions (e.g., irritation or eczema). For this reason in particular, these electrodes should be replaced with dry electrodes [12,13]. Dry sensors work without the use of conductive gel and other skin preparations. However, these sensors depend on the interfacial potential, the contact surface, the high interfacial impedance, and the noise [13]. For bioimpedance measurements, three methods are used: configuration with two electrodes, with three electrodes, and four electrodes, respectively. The four-electrode method has been frequently used to overcome the interference that occurs at the electrode–skin interface, while the method with two-electrodes presents the advantage that it does not require a circuit as complicated as that for measuring the impedance by the four-electrode method [14]. For ECG monitoring, used to detect cardiovascular disease, the bioimpedance electrodes are positioned on the chest, neck, finger or wrist [15]. A category of polarizable electrodes is the orbital electrodes. Dry polarizable orbital electrodes are made to last longer than the common clinical electrodes such as Ag/AgCl. An orbital electrode consists in a mixture of metals like aluminium, gold/gold chloride nickel and titanium and stainless steel. They can cause skin irritation over long-duration use [16,17]. In the last period, the polymers are the most promising organic materials for electronic applications, as stretchable electronic skin and flexible biomedical sensors, due to their valuable properties, like good mechanical deformability and robustness, higher device density, and skin biocompatibility. The polymers can replace the metallic electrodes, which are stiff and uncomfortable for the skin [10,12,18]. Elastomers represent the first class of polymers with applications in bioimpedance electrodes for ECG monitoring, for example, PDMS (polydimethylsiloxane). Chlaihawia, A.A. et al. developed a flexible dry sensor on polyethylene terephthalate PET substrate. A silver electrode was printed was deposited on this PET substrate by the screen printing method. Finally, it was deposited on the printed Ag electrode the composite multi-walled carbon nanotubes (MWCNT)/PDMS, by using a bar coating technique. However, the electrodes presented high impedance values and good linearity of impedance-frequency curve [19,20]. Baek et al. developed a flexible dry sensor for ECG monitoring by depositing gold on PDMS films using a plasma treatment; however, this sensor presents a poor skin-contact electric connectivity [21]. Recently, different conductive polymers, such as polythiophene, polyaniline, and polypyrrole

(PPY), are used in various fields like flexible electronic devices, sensors, catalysis, batteries, supercapacitors, microactuators, anti-electrostatic coatings, low-cost solar cells, and biomedical, due to their excellent electrical conductivity, thermal stability, environmental stability and relative ease of synthesis. These good properties come from their chemical structure, e.g., conjugated electrons or alternating the single bond with a double bond system [22–26]. A conductive polymer used as a bioimpedance electrode can be the composite PEDOT/PSS, poly(3,4-ethylenedioxythiophene):(styrenesulfonic acid), where PSS is used as a doping agent. Karimullaha, A.S. et al. developed a bioimpedance sensor based on PEDOT/PSS, with low impedance, over conventional material such as gold, which is due to the low charge transfer resistance of PEDOT/PSS [27]. Takamatsu, S. et al. developed a bioimpedance sensor based on PEDOT/PSS coated on a fabric characterised by low impedance and long-term stability. However, making the sensor is complex and expensive and presents a poor linearity of the impedance-frequency curve [28]. This polymer was used to achieve the electrode patterns on textiles because it presents a low impedance contact with human skin. From the conductive polymers, the polypyrrole was the most studied, experimented and used in various applications because of its good electrical and electronic properties, good stability derived from its aromatic ring chemical structure, and π -conjugated bonds, which can be modified by oxidation and protonation [29,30]. Conductive polymers are present in a variety of biomedical applications like implants for neural prosthetics [31], biomaterials for biosensors application [32], evaluation of their biocompatibility in nerve tissue in vitro and in vivo [33], as a biomaterial for implants [34], and in studies on the interaction of cells and tissues of polypyrrole [35]. For ECG measurements, Jimenez, O.T. et al. developed a bioimpedance disk sensor with polypyrrole, without no conductive agglutinant, to increase the electrical conductivity of the sensitive material [36].

This paper presents a new dry polarizable bioimpedance sensor based on polypyrrole and silver (Ag) nanoparticles (NPs)/polypyrrole hybrid nanocomposites. Ag NPs were chosen for the functionalisation of polypyrrole for two main reasons: the increase in the sensitive materials' electrical conductivity and its antimicrobial properties [37], respectively.

The advantages of the presented sensors consist of low impedance values in the frequency range of interest for skin bioimpedance monitoring, good linearity of the impedance vs. frequency curve in the same frequency range, and simple realisation without using complex equipment and inexpensive construction. In addition, the paper presents a comparative study of these new sensing materials.

2. Materials and Methods

Pyrrole monomer for synthesis (97% purity and density of 0.967–0.971 g/cm³) was purchased from Merck; FeCl₃ × 6H₂O (99.8%) and AgNO₃ salts, of analytical grade, were purchased from REACTIVUL SA Romania. Deionised water was used as a solvent. The polypyrrole and Ag Np/polypyrrole composites synthesis follow the path described in reference [17].

2.1. Polypyrrole Synthesis

PPY was synthesised using a chemical oxidative polymerisation method using pyrrole monomer and FeCl₃ × 6H₂O as an oxidative agent (Figure 1). Briefly, a solution of 0.05 M pyrrole monomer was added, over 45 min, dropwise, in a solution of 0.115 M FeCl₃ × 6H₂O, under stirring at room temperature (the ratio of monomer/ FeCl₃ × 6H₂O was 1/2.33). The mixture was slowly stirred for another 4 h. After that, the solution was left at room temperature for 24 h without mixing. Monomer pyrrole's polymerisation reaction with an aqueous solution of FeCl₃ × 6H₂O is a fast reaction to obtain a black precipitate [38]. The black precipitate formed was filtered and washed with deionised water and dried for 24 h at room temperature, followed by drying at 80 °C for 10 h. The oxidative polymerisation reaction of pyrrole in the presence of oxidative agent FeCl₃ × 6H₂O is described by the following reaction [30,36,38] (1).

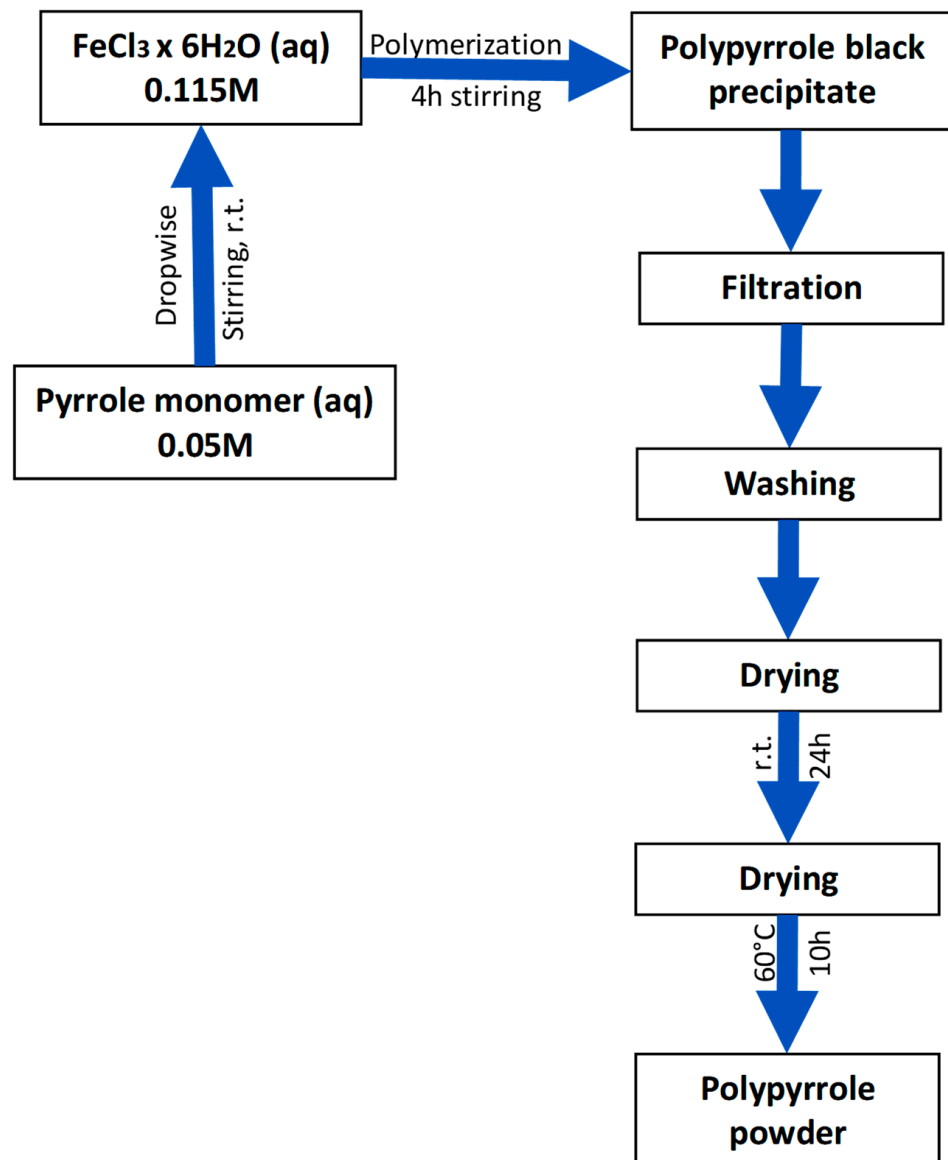
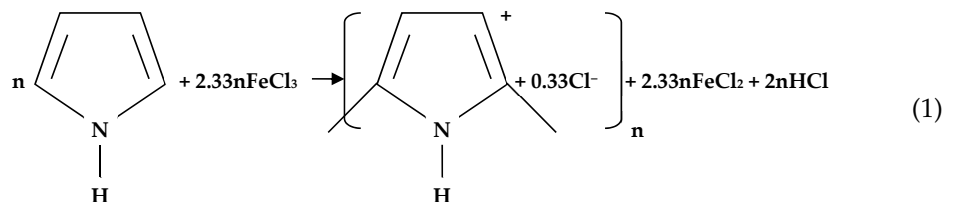


Figure 1. The flow stages of the polypyrrole (PPY) synthesis.



The flow of the synthesis stages of the sensitive material polypyrrole is presented in Figure 1.

2.2. Ag NP/PPY Hybrid Nanocomposite Synthesis

The Ag NPs were obtained following a chemical synthesis route by reducing a solution of AgNO_3 with hydrazine (the ratio of AgNO_3 /Hydrazine was 1/3) at a temperature of 80°C . The pale-yellow colloidal silver solution was mixed with a fresh solution of pyrrole monomer/ $\text{FeCl}_3 \times 6\text{H}_2\text{O}$, following the same steps as the polypyrrole synthesis described

above (Figure 2). Thus, two composites of 10% and 20% (w/w) of Ag Np in polypyrrole were obtained.

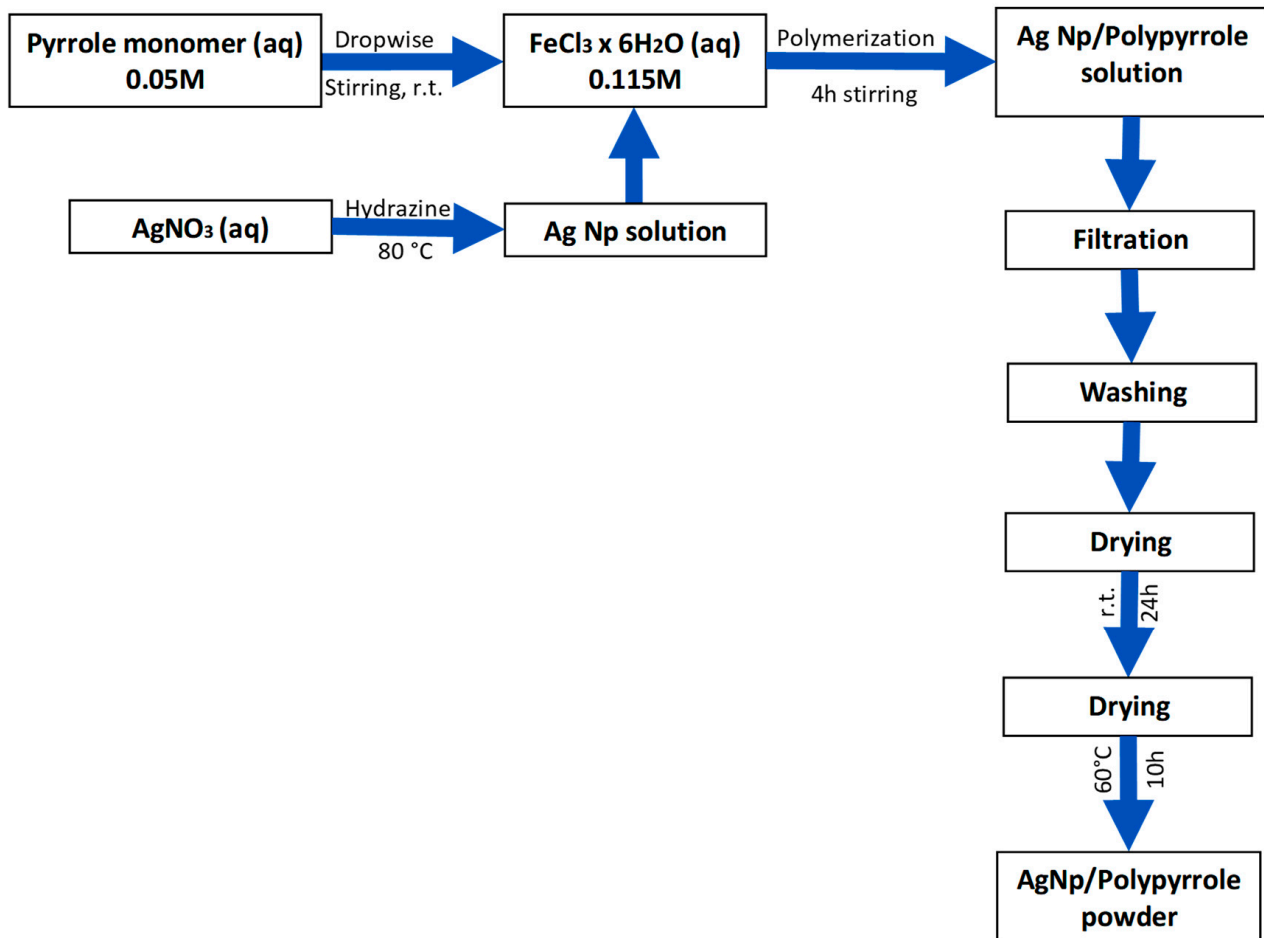


Figure 2. The flow stages of Ag/PPY hybrid nanocomposites synthesis.

2.3. Obtaining the Dry Polarizable Electric Bioimpedance Sensors

In making the bioimpedance electrodes, the polypyrrole and Ag/polypyrrole hybrid nanocomposite powders were pressed in disk format, with 6 tons force/cm² pressure, by using a hydraulic press: Ø 12 mm ± 0.2 mm, h = 1.6 ± 0.3 mm for PPY and Ø 12 mm ± 0.2 mm, h = 2.5 ± 0.3 mm for Ag NPs/PPY nanocomposite. A layer of conductive silver paste was deposited on one side of the obtained disks. Each of the disks thus obtained are arranged on another silver disk of the same diameter. The dry polarizable electric bioimpedance sensor (Figure 3) was obtained by using two electrodes arranged at 6 cm from each other.

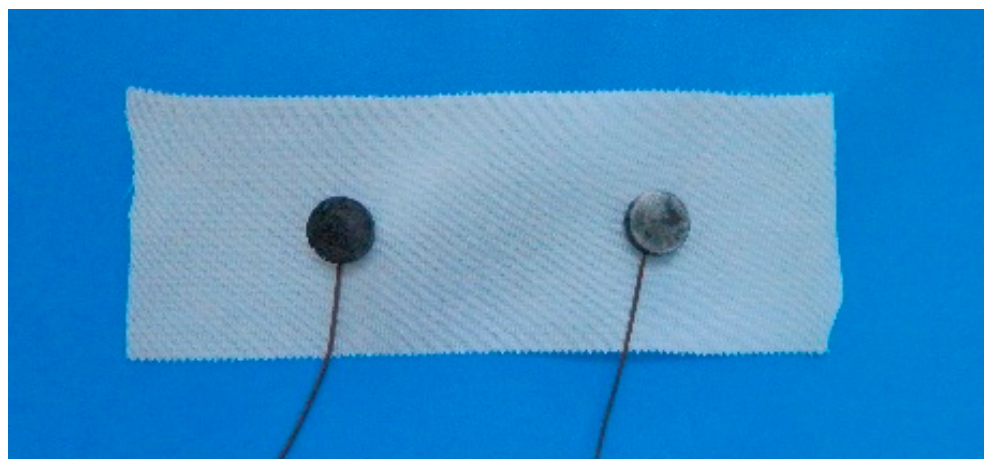


Figure 3. Image of the dry polarizable electric bioimpedance sensor made by using Ag/PPY hybrid nanocomposites as the sensing material.

The electrical connection is made from the opposite side of the silver disk.

2.4. Equipment

The structures of PPY and Ag NPs/PPY hybrid nanocomposites were studied by attenuated total reflection Fourier transform infrared (ATR-FTIR) spectroscopy using a spectrometer Jasco 4200 coupled with an ATR JASCO PRO 470–H accessory. The samples were measured directly by placing them on the ATR device's crystal and pressing with a controlled force, in the following conditions: the spectral range of $4000\text{--}500\text{ cm}^{-1}$, resolution 4 cm^{-1} , scans number/spectrum: 50 accumulations. Raman spectroscopy measurements were performed with a Raman-dispersive spectrometer–LabRam HR Evolution, Horiba Jobin Yvone, France, equipped with laser extinction of 633 nm, acquisition time 15 s, and 100 accumulation/spectrum. The Raman spectra were used to characterise the disorder degree in the synthesised nanocomposite. The morphology of the samples PPY and Ag NPs/PPY nanocomposite was studied by scanning electron microscopy (SEM) using a Carl Zeiss SMT FESEM-FIB (Scanning Microscope Tunnelling Field Emission Scanning Electron Microscope-Focused Ion Beam) Auriga type scanner in the following conditions: the tension of acceleration 10 kV and magnitude of 20 and 50 k. The elemental analysis (energy-dispersive X-ray spectroscopy (EDX)) was performed with a dispersive energy probe of Inca Energy 250 type Oxford Instruments Ltd. England coupled to SEM. The electric bioimpedance measurements were carried-out with a precision LCR (Inductance Capacitance Resistance) meter, AGILENT E4980 A type, in the frequency range of 1–300 kHz. The configuration was in two points measurement, the simplest set-up method for electric bioimpedance measurements [4], by using a bioimpedance sensor made of the two obtained electrodes (Figure 3).

3. Results

3.1. Structural Characterisation

3.1.1. Raman Spectroscopy

Figure 4 shows the Raman spectra recorded on the three sensitive materials. The most important band in the Raman spectra for pyrrole is the one present around 1605 cm^{-1} , representing the vibration mode characteristic of the C=C bonds, which form the skeleton of the polypyrrole [39]. The Raman spectrum shows an increase of the band intensity, positioned at around 1605 cm^{-1} , with the amount of silver, which concludes that the increase of the percentage of silver causes modifications of the crystalline structure of the polypyrrole. The second important group of bands appears at 1321 cm^{-1} and 1331 cm^{-1} , attributed to the pyrrolic ring's stretching mode. The third important group of bands appears at $1040\text{--}1054\text{ cm}^{-1}$, determined by the C–H bond's plane deforma-

tion. Also, it can be observed that the intensity of the bands at $1321\text{--}1331\text{ cm}^{-1}$ and $1040\text{--}1054\text{ cm}^{-1}$ increases with the amount of silver (Ag). The introduction of silver (Ag) determines the polypyrrole's amorphisation, deformation of the pyrrole ring, and the C–H bond [39]. The introduction of a large quantity, respectively of 20% Ag, leads to the disruption of the polypyrrole's internal structure, reducing its crystallinity.

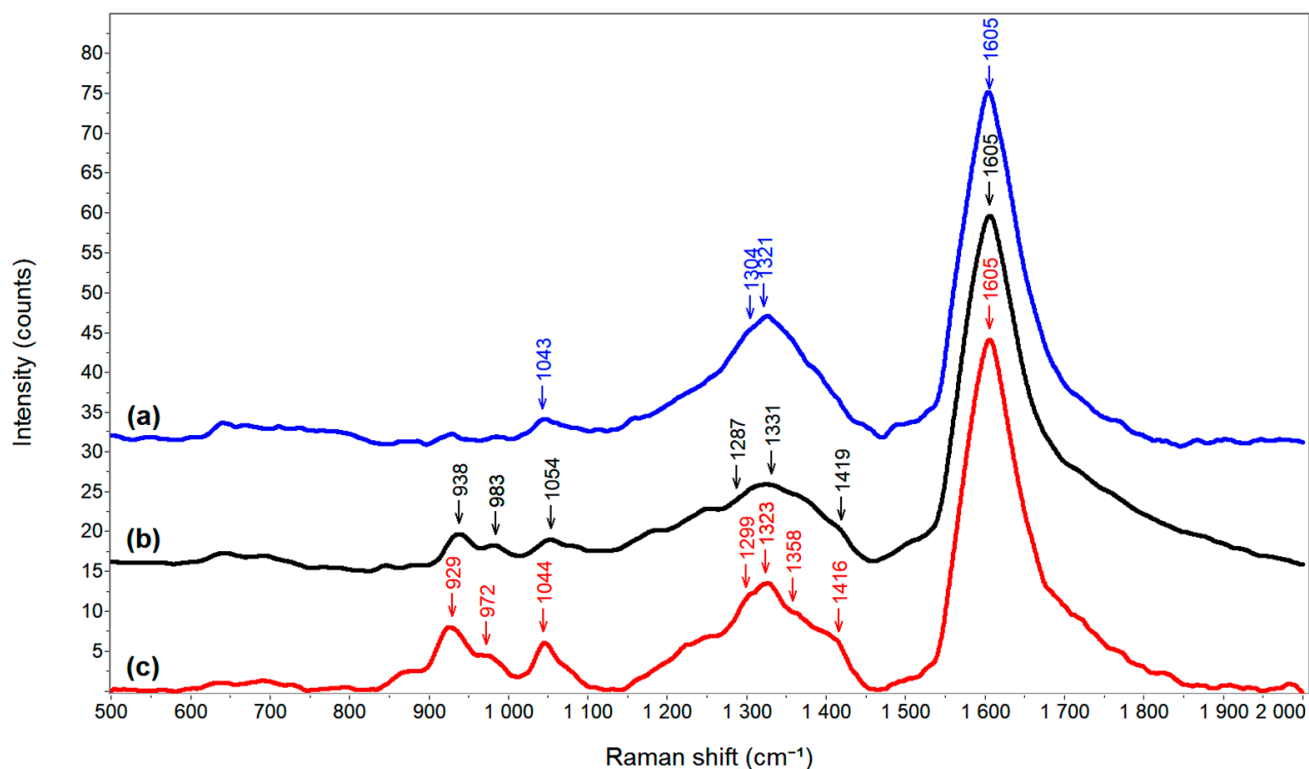


Figure 4. Raman spectra recorded on: (a) PPY; (b) 10%Ag/PPY; (c) 20%Ag/PPY.

3.1.2. Fourier Transform Infrared (FTIR) Spectroscopy

The molecular structures of synthesised polypyrrole and nanocomposites with 10% and 20% silver (Ag) embedded into polymer matrix were analysed using FTIR spectroscopy (Figure 5). The allure of the obtained FTIR spectra confirms the structural configuration of the PPY indicated from the literature data: the peak at 780 cm^{-1} attributed to C–H out of plane of the polypyrrole ring, the peak at 1040 cm^{-1} represents N–H in plane deformation [40], the peak located at 1186 cm^{-1} is assigned to C–N stretching vibration [41]. The peaks at 1288 cm^{-1} and 1040 cm^{-1} are assigned to C–N in plane vibration; the peak at 1557 cm^{-1} is attributed to the polypyrrole ring's vibration [41,42]. The broad peak at 3228 cm^{-1} is attributed to the stretching of N–H and C–H bonds [43,44]. The Ag NPs' introduction into the PPY structure leads to some PPY FTIR characteristic bands' displacements, indicating specific interactions between Ag NPs and the PPY functional groups, especially those in the N–H group region [43,45].

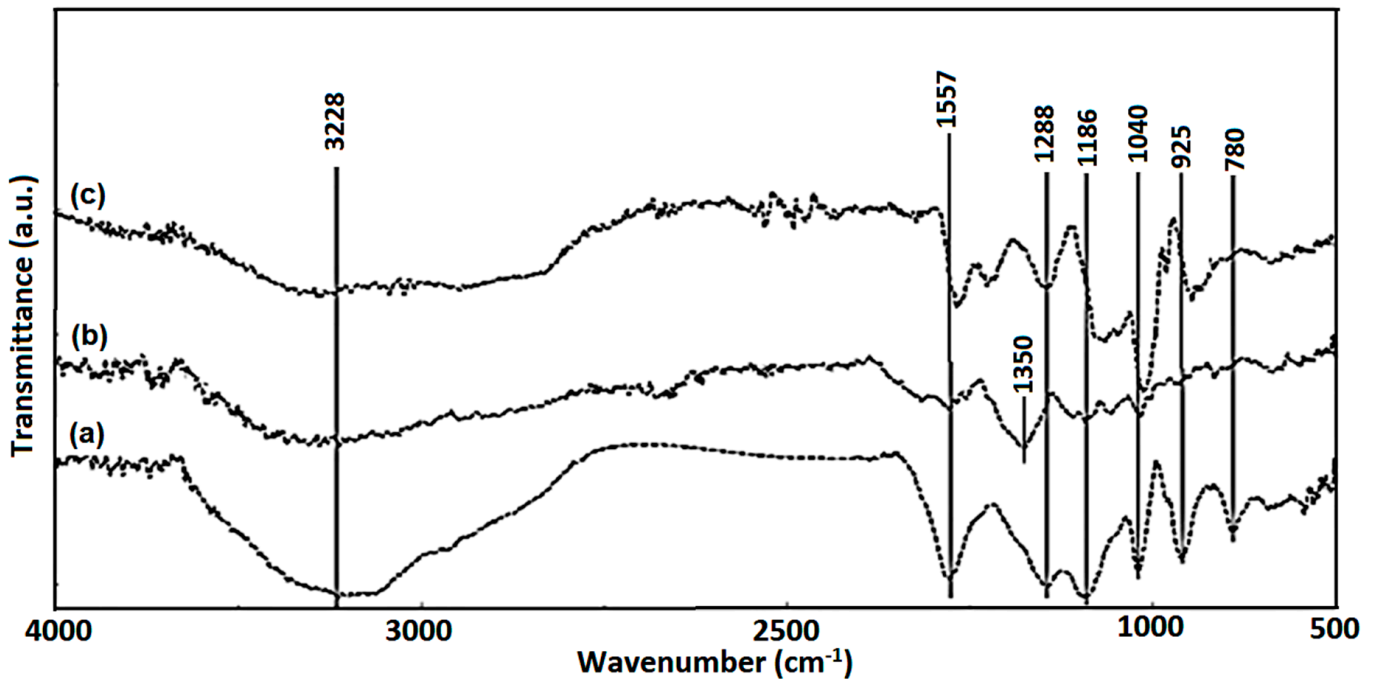


Figure 5. Fourier transform infrared (FTIR) spectra recorded on: (a) PPY; (b) 10%Ag/PPY; (c) 20%Ag/PPY.

3.2. The Morphological Analysis

The morphological structure of the three sensor materials was undertaken by SEM microscopy (Figure 6). The SEM images show a classic polypyrrole structure consisting of globular units with average dimensions around 400 nm formed by the collision of smaller globular formations with average dimensions around 200 nm. In the case of the 10%Ag/PPY hybrid nanocomposite (Figure 6b), a classical structure is observed, mainly globular but with smaller dimensions than in the case of simple PPY. In addition, an inhomogeneous dispersion of Ag NPs clusters can be observed on the PPY surface. These non-homogeneous silver clusters have submicron sizes, formed of particles with wurtzite crystalline structure (parallelepiped with a height of 200–300 nm and widths of 100 nm (Figure 6c)). In the case of the 20%Ag/PPY hybrid nanocomposite, the structure is similar to the one previously presented. In both cases, the PPY covers the silver nanoparticles, as in the core-shell structure.

3.3. Elemental Analysis

The backscattered electron images, the spectra and elemental mapping for the samples PPY, 10%Ag/PPY and 20%Ag/PPY (Figures 7–9) confirms the presence of C, N, Cl and O for all analysed materials and of Ag for 10%Ag/PPY and 20%Ag/PPY hybrid nanocomposites, which confirms the incorporation of Ag into the polymer PPY phase. For all samples, EDX mapping shows a relative homogeneous distribution of C, N, Cl, and O, but for Ag, some aggregates distribution in composites, much more distinguished in the sample with 20%Ag/PPY, is observed.

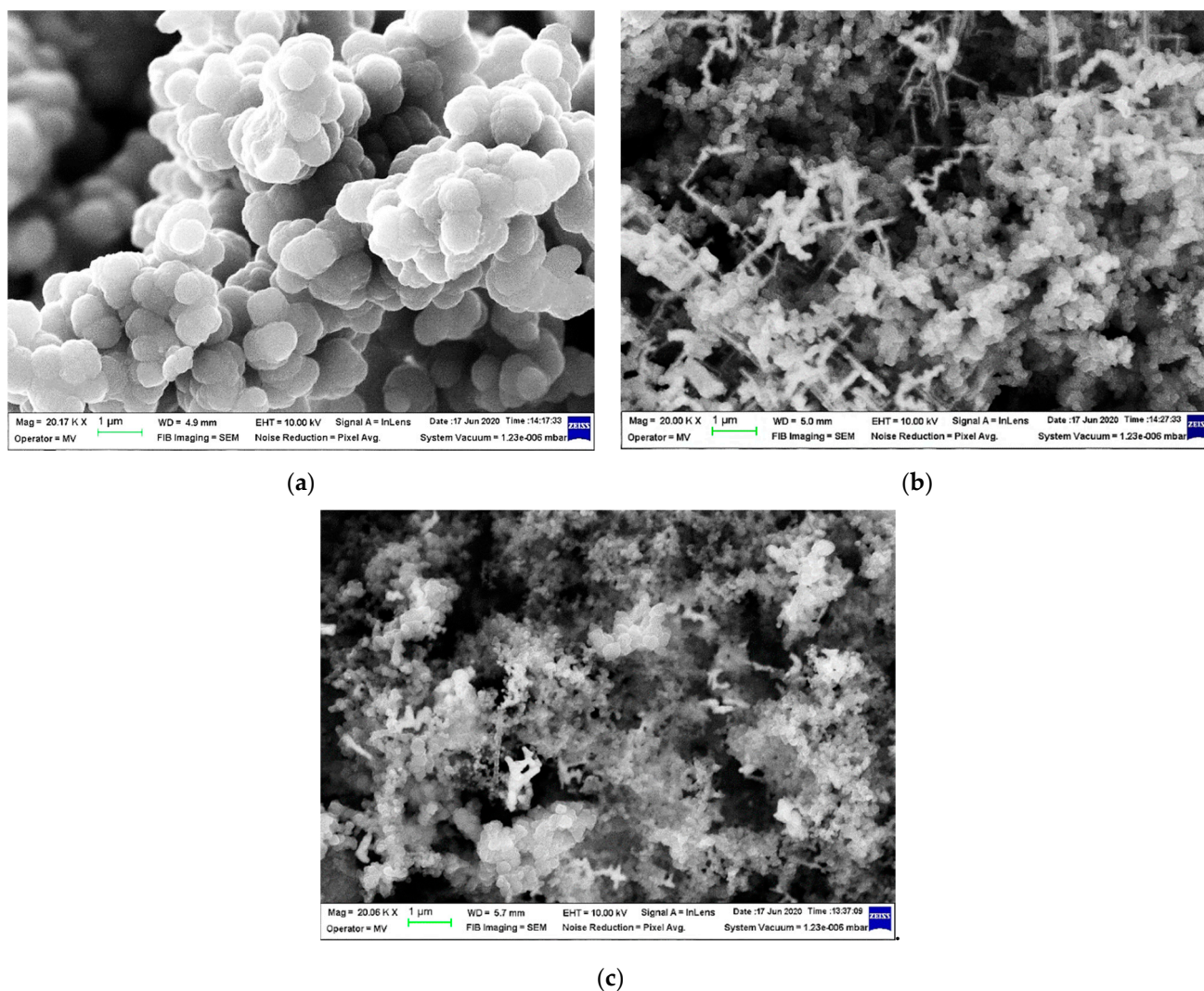


Figure 6. Scanning Electron Microscopy (SEM) images recorded on: (a) PPY; (b) 10%Ag/PPY; (c) 20%Ag/PPY.

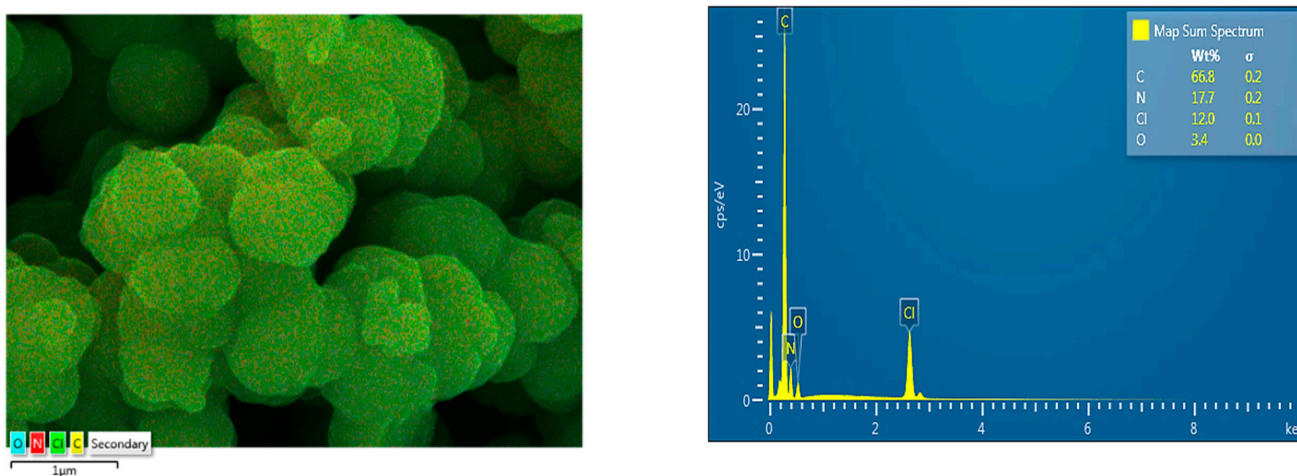


Figure 7. Energy-dispersive X-ray spectroscopy (EDX) elemental mapping for distribution of C, N, O and Cl in PPY.

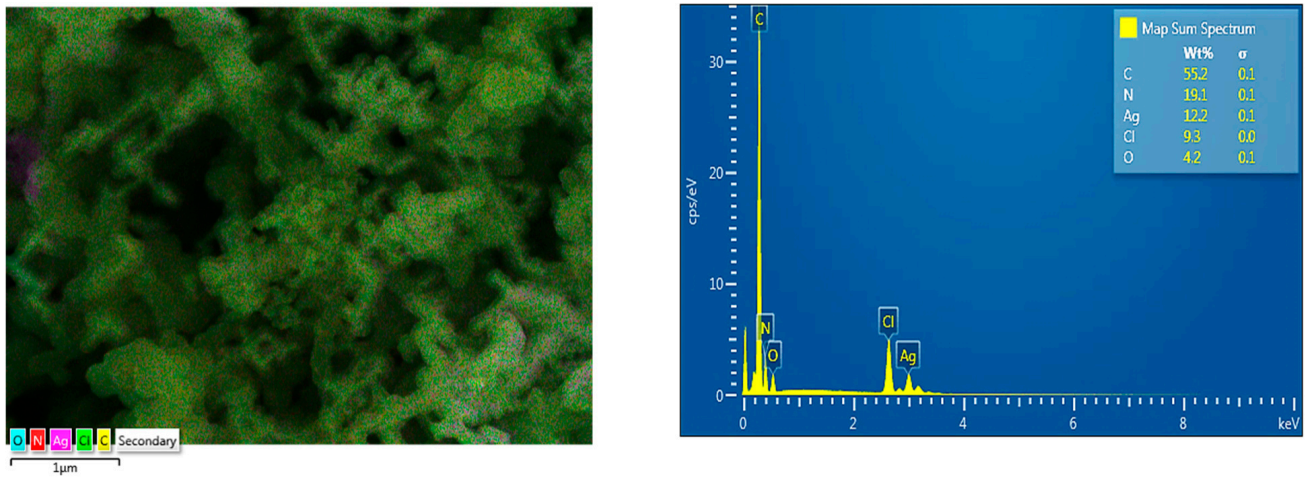


Figure 8. EDX elemental mapping images for C, N, O, Cl and Ag in 10%Ag/PPY hybrid nanocomposite.

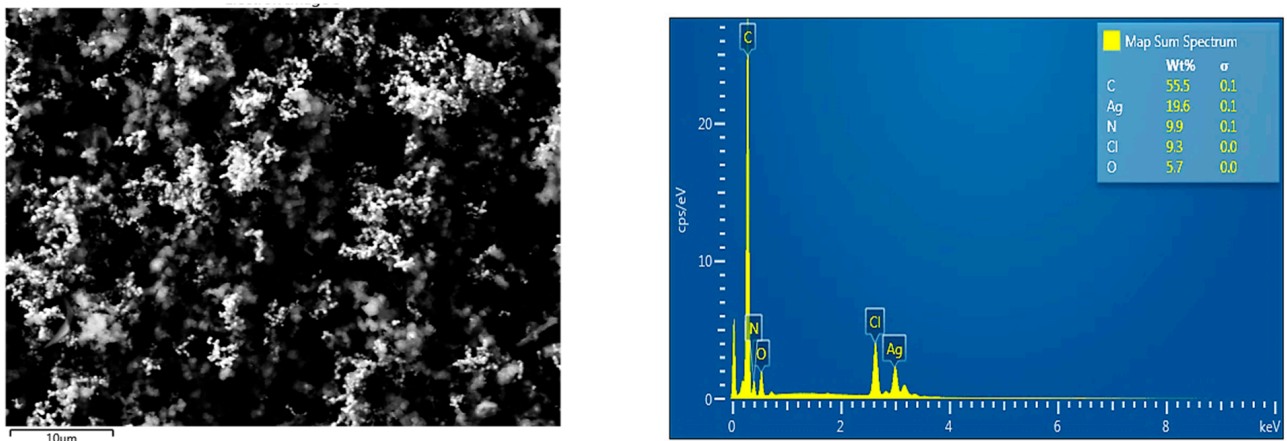


Figure 9. EDX elemental mapping images for C, N, O, Cl and Ag in 20%Ag/PPY hybrid nanocomposite.

3.4. Measurements of Magnitude Level of Skin Bioimpedance

The dry polarizable electric bioimpedance sensors is realized by using two electrodes. These two electrodes were glued on an adhesive strip for bioimpedance measurements and spaced at 6 cm apart from each other (Figures 3 and 4). The equivalent parallel scheme Rpe-Cpe (Resistance-Capacity) corresponding for electrodes is shown in Figure 10.

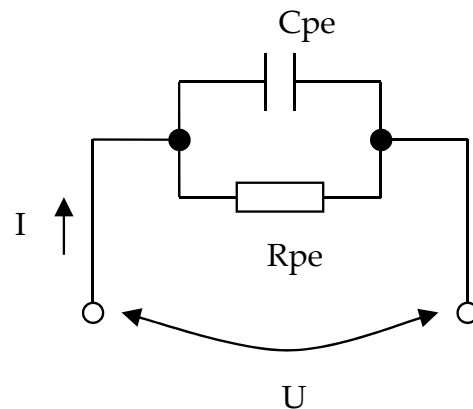


Figure 10. Equivalent parallel scheme Rpe-Cpe (Resistance-Capacity) corresponding for electrodes.

For electrical impedance measurements of electrode with frequency, disk-shaped electrodes were silvered with silver paste on both sides, as shown in Figure 11.

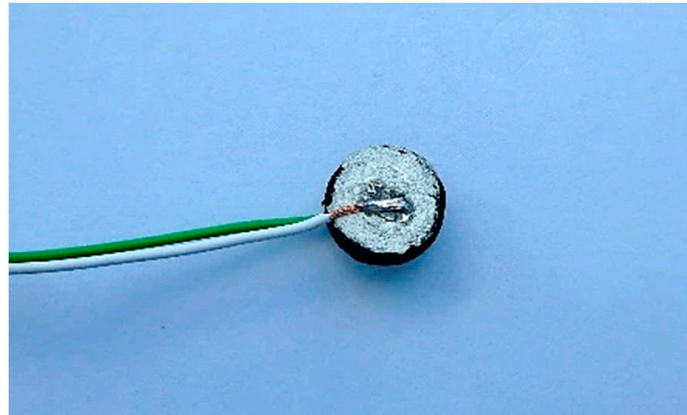


Figure 11. Disk-shaped electrode made with sensitive materials PPY or hybrid nanocomposite 10%Ag/PPY or hybrid nanocomposite 20%Ag/PPY, silvered with silver paste on both sides.

Table 1 shows electrical impedance Z_e , in terms of magnitude level and the Cpe capacity and Rpe resistance respectively of the electrode. The values of measurements obtained is corresponding to the equivalent parallel Rpe-Cpe scheme for electrodes (Figure 10). The obtained data is corresponding for three electrodes made with sensitive materials PPY and hybrid nanocomposites 10%Ag/PPY and 20%Ag/PPY, respectively. The measurements of electric impedance of electrode were performed at an applied sinusoidal voltage of 2 Vpeak-peak, for the frequency range of 10–300 kHz and at a temperature of 25 °C, by using a precision LCR meter, AGILENT E4980 A type. It can be seen that the electrodes made with hybrid nanocomposites 10%Ag/PPY and 20%Ag/PPY as sensitive materials have a good linearity of the impedance vs. frequency in the frequency range of 10–300 kHz (Figure 12). In addition, the value of electric impedance of electrodes made with hybrid nanocomposites 10%Ag/PPY and 20%Ag/PPY is quasi-constant with frequency (Figure 12).

Table 1. The measurements of electrical impedance of electrode Z_e , of capacity Cpe and Rpe resistance respectively.

Frequency, [kHz]	Electrode of PPY			Electrode of 10%Ag/PPY			Electrode of 20%Ag/PPY		
	Cpe, [nF]	Rpe, [Ω]	Impedance Z_e , [Ω]	Cpe, [nF]	Rpe, [Ω]	Impedance Z_e , [Ω]	Cpe, [nF]	Rpe, [Ω]	Impedance Z_e , [Ω]
10	2.484	392.5	488.8	2.542	138.5	143.2	2.444	103.4	102.84
50	2.082	382.9	451.4	1.827	139.5	141.88	2.130	102.8	102.14
100	1.925	363.4	392.25	1.682	137.8	139.02	2.033	102.04	100.94
120	1.899	355.1	370	1.648	136.54	137.7	2.011	102.31	100.17
150	1.825	343.7	339.37	1.634	135.4	135.68	1.985	101.70	99.22
200	1.749	323.6	296.93	1.583	133.5	131.98	1.948	100.75	97.10
250	1.695	304.47	263.3	1.540	131.45	128.02	1.920	99.54	94.7
300	1.637	286.61	236.59	1.510	129.64	124	1.894	98.25	92.15

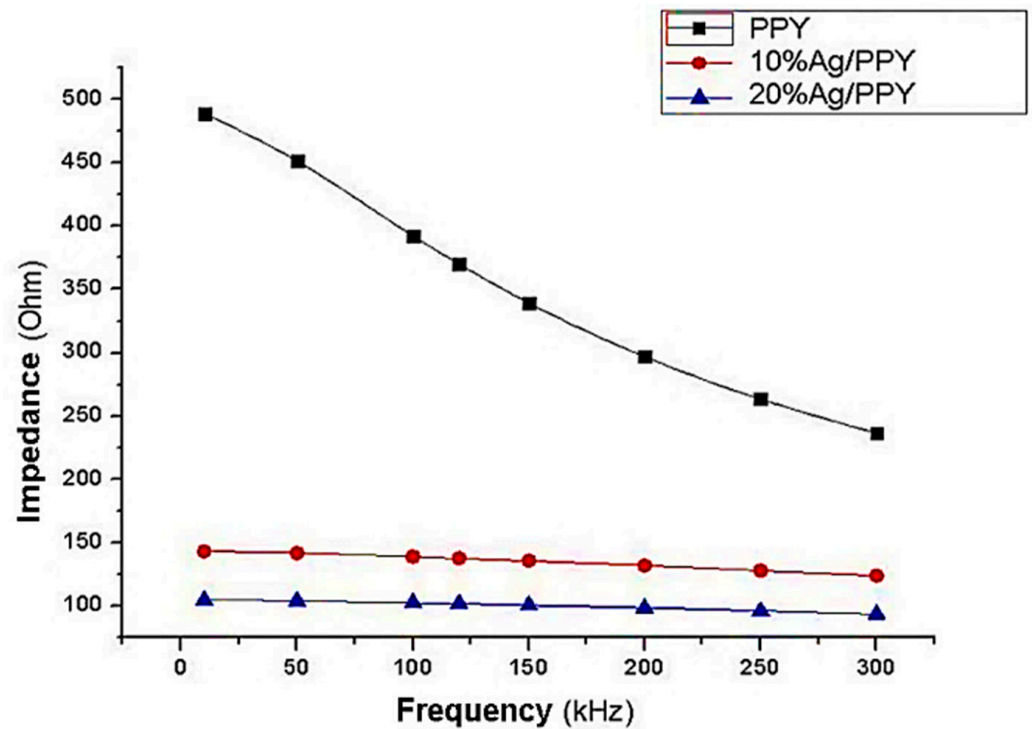


Figure 12. Variation of electric impedance of electrodes with frequency, for electrodes that is realised with sensitive materials PPY and hybrid nanocomposites 10%Ag/PPY and 20%Ag/PPY, respectively.

The measurement of magnitude of the level of skin bioimpedance in series with of two electrodes' impedance can be performed at two points, by using the dry polarizable electric bioimpedance sensor.

For the magnitude level of total bioimpedance measurements, i.e., skin bioimpedance in series with two electrodes' impedance, six subjects participated, three men with the initials, LPD, RC, CO with ages between 32 and 59 years old, and three women with the initials FB, CB, II, with ages between 43 and 52 years old. The dry bioimpedance sensor was attached distally on the left wrist along with the radial artery (Figure 13).



Figure 13. The used test bench image for total bioimpedance measurements and dry polarizable bioimpedance sensor location on the arm of the subject.

The magnitude level of total bioimpedance measurements, i.e., for skin bioimpedance in series with two electrodes' impedance were achieved with the subjects in the sitting position on the same day for each subject. In a first stage, for all the six subjects selected, the impedance was measured only with PPY and 20%Ag/PPY composite bioimpedance sensors, in the frequency range of 1–300 kHz. In Table 2 the experimental data are presented.

Table 2. The measurements of magnitude level of total bioimpedance, i.e., for skin bioimpedance in series with two electrodes impedance, the data is corresponding for the two bioimpedance sensors made with sensitive materials: PPY and 20%Ag/PPY hybrid nanocomposite.

Frequency, [kHz]	LPD 59 Years Old		RC 32 Years Old		CO 50 Years Old		FB 43 Years Old		CB 52 Years Old		II 46 Years Old	
	Impedance, [kΩ]		Impedance, [kΩ]		Impedance, [kΩ]		Impedance, [kΩ]		Impedance, [kΩ]		Impedance, [kΩ]	
	PPY	20%Ag/PPY	PPY	20%Ag/PPY	PPY	20%Ag/PPY	PPY	20%Ag/PPY	PPY	20%Ag/PPY	PPY	20%Ag/PPY
1	16	41	65.70	450	16	100	80	220	155	380	58.70	380
10	3.87	12	12.70	54.8	3.55	18.20	15.54	31.30	24	43	13.04	38.80
50	1.82	3.24	4.23	12.9	1.82	4.75	5.30	7.20	7.12	10	5.02	8
100	1.42	2.00	2.57	7.01	1.40	2.60	3.37	3.91	4.21	4.80	3.24	4.02
120	1.31	1.70	2.27	6.04	1.30	2.20	2.95	3.42	3.60	4.60	2.76	3.25
150	1.18	1.47	1.97	4.75	1.17	1.81	2.52	2.75	3	3.52	2.34	2.54
200	1.00	1.04	1.65	4.12	1.02	1.40	2.09	2.11	2.34	2.71	1.88	1.87
250	0.90	0.88	1.44	3.24	0.88	1.17	1.75	1.84	1.92	2.25	1.58	1.54
300	0.82	0.79	1.23	3.07	0.80	1	1.52	1.44	1.67	1.80	1.36	1.30

In the case of the PPY bioimpedance sensor, the total bioimpedance decreases with frequency (Figure 14), and this decrease is more significant in the case of male subjects than female subjects. Thus, at the low frequency of 1 kHz, the total bioimpedance values in the case of the male subjects were between 16–65.70 kΩ much lower values compared to 58.7–155 kΩ in the case of the female subjects; it is possible that the skin of the male is more conductive than the skin conductivity of females. In the case of the 20%Ag/PPY hybrid nanocomposite sensor, the same tendency of decreasing the total bioimpedance with frequency is observed, but compared to neat PPY, the total bioimpedance values are increased due to Ag NPs incorporated in the polymer chain and obstruction of polymer electron gaps.

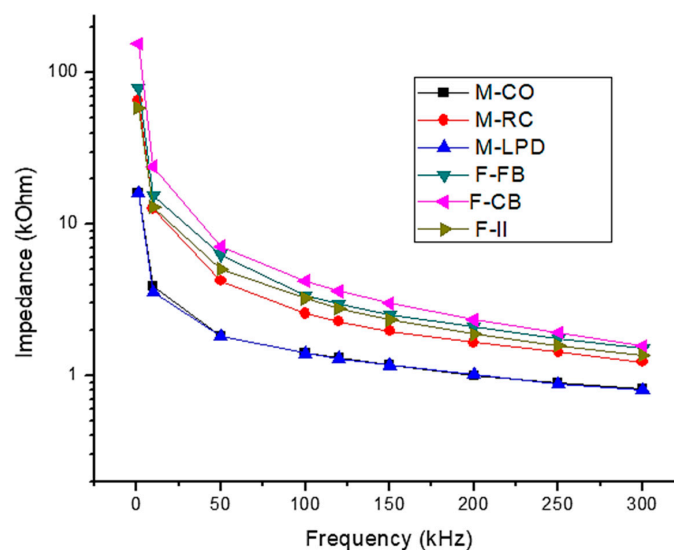


Figure 14. The magnitude of total electric bioimpedance versus frequency measurements of PPY bioimpedance sensor for all subjects.

Moreover, the measurements performed to obtain variation of electric impedance of electrodes with frequency (Figure 12) shows the influence of Ag NPs incorporated in the polymer. On that account for electrodes realised with the sensitive material PPY, the impedance of electrode was in the range of 236.59–488.8 Ω while for electrodes that realised with hybrid nanocomposites 10%Ag/PPY was in the range of 124–143.2 Ω and in the range of 92.15–102.84 Ω for hybrid nanocomposites 20%Ag/PPY.

In addition, the total bioimpedance values obtained at a low frequency of 1 kHz are increased in the case of female subjects, with values between of 220–380 k Ω compared to those of the male subjects between of 41–100 k Ω , except for a single male whose total bioimpedance value is 450 k Ω (Figure 15). The same tendency was observed for measurements performed at 300 kHz.

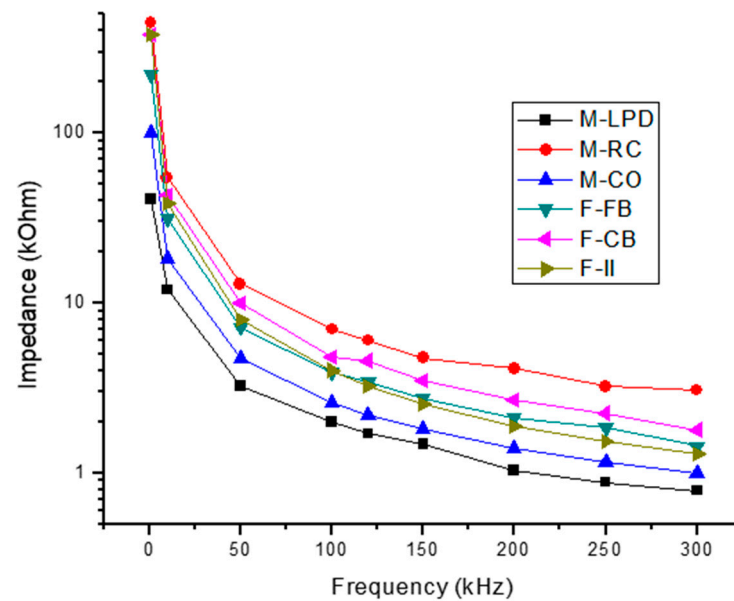


Figure 15. The magnitude of total electric bioimpedance versus frequency measurements of 20%Ag/PPY nanocomposite bioimpedance sensor for all subjects.

Table 3 presents the experimental data regarding the total electric bioimpedance variation with frequency for three of the subjects, a man (LPD) and two women (CB and FB). For comparison, the measurements were taken by using three bioimpedance sensors made with sensitive materials: PPY and 10%Ag/PPY and 20%Ag/PPY hybrid nanocomposites.

In this case, a decrease of the total bioimpedance with frequency for all the three human subjects tested (Table 3) was observed. On the frequency domain tested of 1–300 kHz, a more pronounced decrease is found at high frequencies (250–300 kHz), especially for the bioimpedance sensor made with sensitive material 10%Ag/PPY nanocomposite, compared to bioimpedance sensors made with PPY and 20%Ag/PPY nanocomposite. Values of 16–220 k Ω for 1 kHz to 1.80–0.512 k Ω for 300 kHz were observed. At the frequency of 300 kHz, the lowest bioimpedance values were obtained, respectively 0.512 k Ω for men LPD, 1.44 k Ω and 1.33 k Ω for women CB and FB. These trends are also illustrated in Figures 16–18.

Table 3. The measurements of magnitude level of total bioimpedance, i.e., for skin bioimpedance in series with two electrodes impedance, the data is corresponding for three bioimpedance sensors made with sensitive materials: PPY and 10%Ag/PPY and 20%Ag/PPY hybrid nanocomposites.

Frequency, [kHz]	Impedance, [k Ω] Subject 1 LPD			Impedance, [k Ω] Subject 2 CB			Impedance, [k Ω] Subject 3 FB		
	PPY	10%Ag/PPY	20%Ag/PPY	PPY	10%Ag/PPY	20%Ag/PPY	PPY	10%Ag/PPY	20%Ag/PPY
1	16	31.40	41	155	174	380	80	164	220
10	3.87	6.41	12	24	25.80	43	15.54	25.70	31.30
50	1.82	1.87	3.24	7.12	6.64	10	5.30	6.40	7.20
100	1.42	1.10	2	4.28	3.64	4.80	3.37	3.53	3.92
120	1.31	0.944	1.70	3.60	3.07	4.60	2.95	2.38	3.42
150	1.18	0.796	1.47	3	2.52	3.52	2.52	2.05	2.75
200	1.00	0.661	1.04	2.34	1.98	2.71	2.09	1.87	2.11
250	0.90	0.571	0.88	1.92	1.67	2.25	1.75	1.55	1.84
300	0.82	0.512	0.79	1.67	1.44	1.80	1.52	1.33	1.44

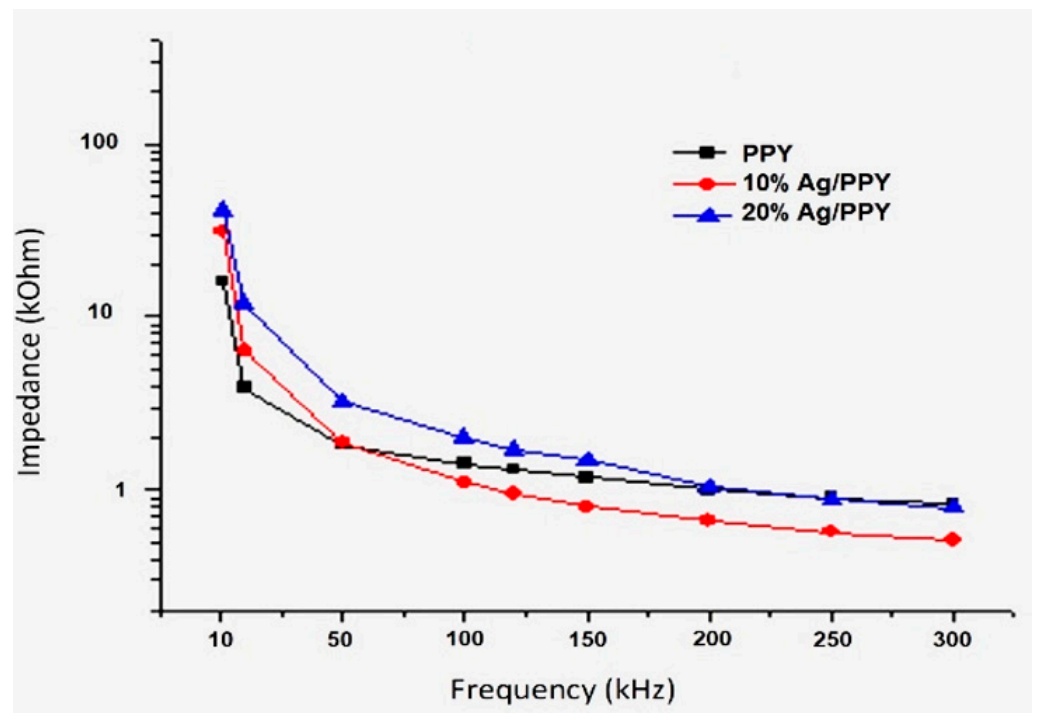


Figure 16. The magnitude of total electric bioimpedance versus frequency for all bioimpedance sensors for subject LPD.

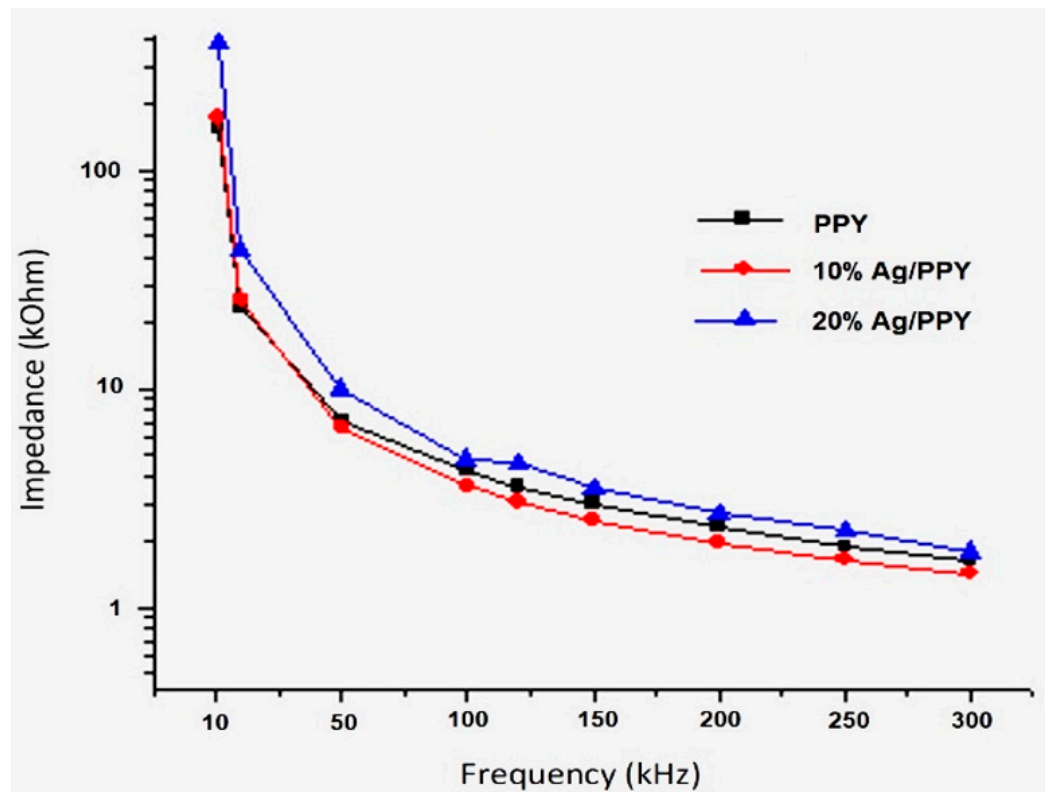


Figure 17. The magnitude of total electric bioimpedance versus frequency for all bioimpedance sensors, for subject CB.

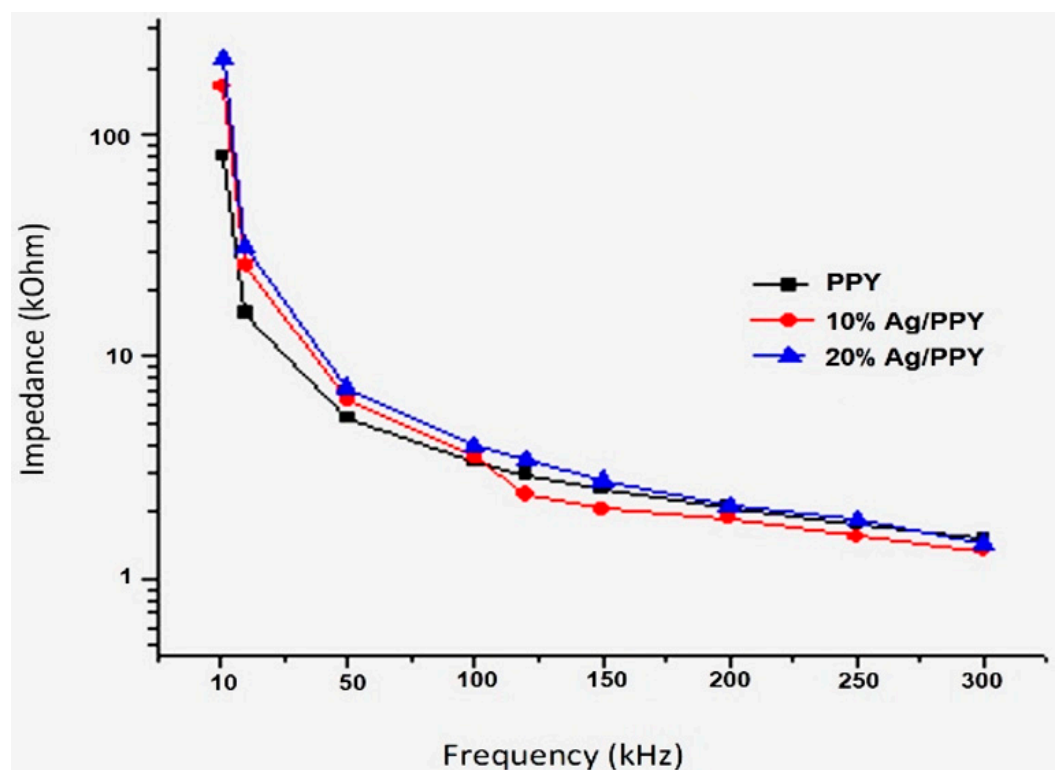


Figure 18. The magnitude of total electric bioimpedance versus frequency for all bioimpedance sensors for subject FB.

In addition, it is worth mentioning that on the analysed frequency range, were observed lower bioimpedance values for the male subjects compared to the bioimpedance values obtained for the female subjects, resulting in a different behaviour between the two sexes in terms of bioimpedance.

A comparative evaluation of results with the literature considered another polymeric material, namely PDMS [46]. A flexible dry electrode for long-term EEG measurement based on PDMS material was realised and tested. The magnitude of total electric bioimpedance was measured by using two electrodes were placed on skin separately (about 3 cm), and then current is applied to measure impedance (Figure 19). The signal of LCR meter is set to 2 V and the frequency range of 20 Hz–10 kHz. In this study, 10 tests on five different participants are performed [46].

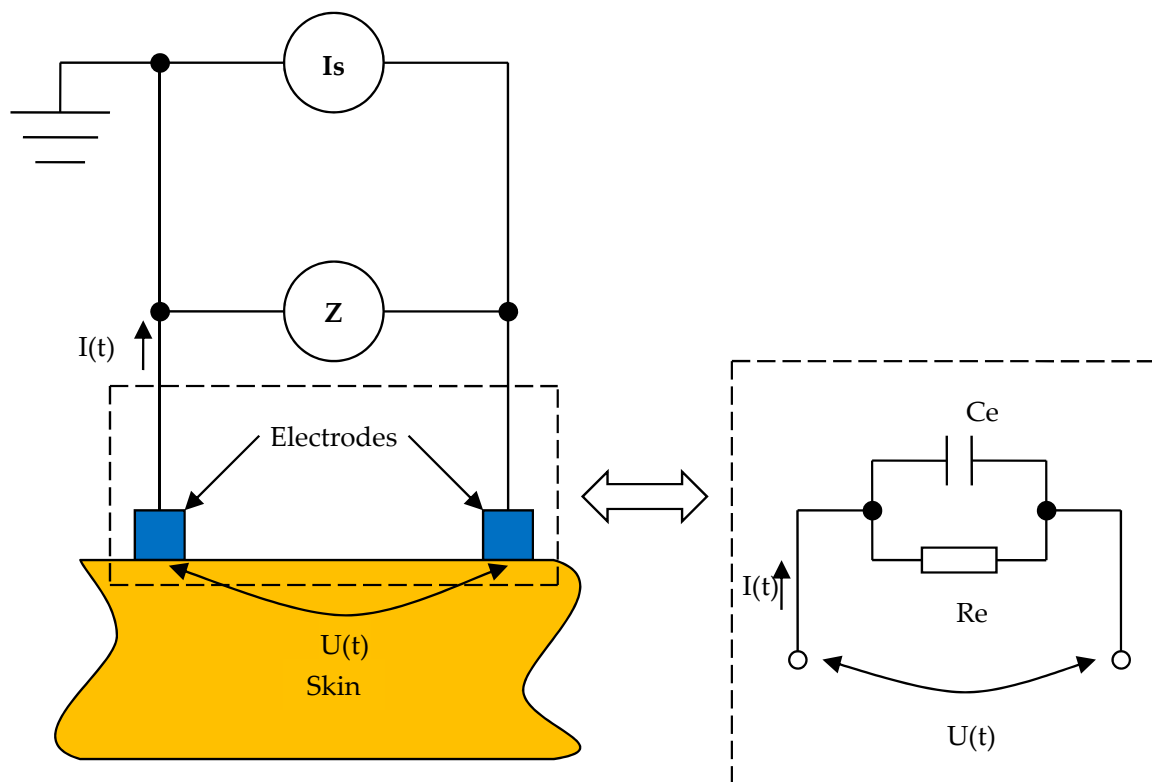


Figure 19. Schematic diagram of measurement circuit for magnitude of total electric bioimpedance versus frequency (adapted from [46]).

The results of these measurements are shown in Figure 20.

Both AgNPs/PPY hybrid nanocomposites as well as PDMS presented a tendency to decrease with frequency of the measured skin bioimpedance. Due to the obstruction of the polymer electron gaps by Ag NPs, the bioimpedance values in the frequency range of 1–300 kHz were higher compared to the behaviour of PDMS in the frequency range of 20 Hz–10 kHz. For both hybrid nanocomposites 10%Ag/PPY and 20%Ag/PPY as well as for PDMS the results obtained indicated a good tendency of quasi-linear decreasing of the electric skin bioimpedance with frequency.

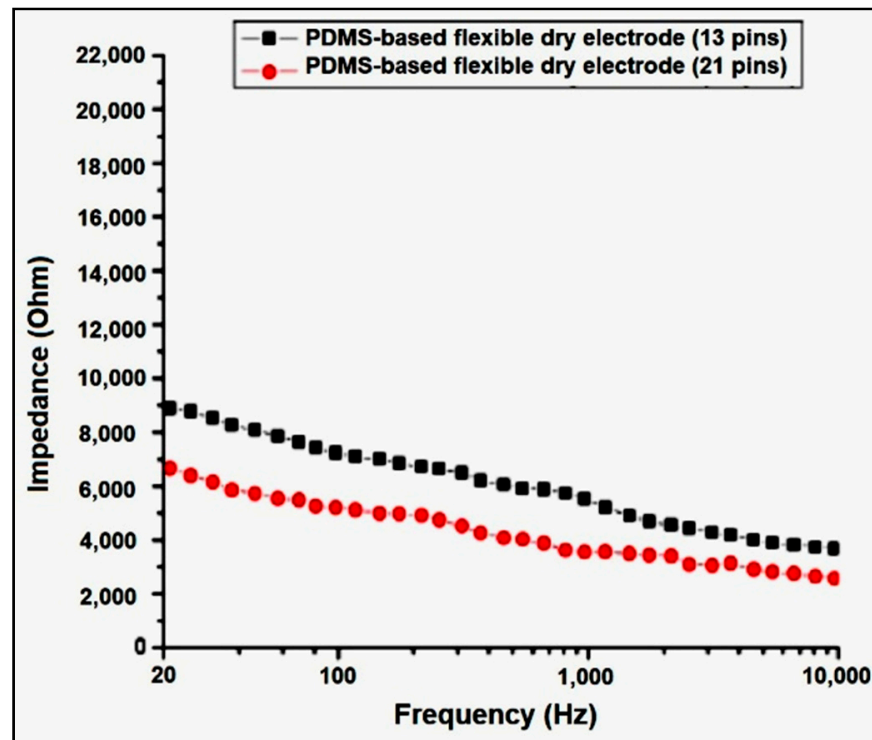


Figure 20. Impedance fluctuation of polydimethylsiloxane (PDMS)-based flexible dry electrode with different area (13 pins, 16.59 cm² and 21 pins, 10.27 cm²) on forehead (adapted from [46]).

4. Conclusions

This paper presents three types of dry polarizable bioimpedance sensors, based on conductive polymer, PPY and hybrid nanocomposite PPY-Ag, with 10 and 20% Ag incorporated in the PPY matrix as sensitive materials, developed for electric bioimpedance measurements.

The conductive polymer PPY was synthesized by chemical oxidative polymerization using $\text{FeCl}_3 \times 6\text{H}_2\text{O}$ like oxidizing agent in molar ratio polymer/oxidizing agent 1:2.33. For hybrid composites synthesis Ag/PPY, the colloid solution of Ag NPs was introduced in the pyrrole solution, followed by polymerization.

The structure and morphology of the sensitive materials were assessed through a series of investigative methods, and it was found that the introduction of Ag NPs in the PPY leads to the formation of silver clusters covered by PPY, similar to a core-shell structure. In addition, an amorphization of the polypyrrole should be considered in the presence of Ag NPs. From Raman spectra are resulted that a first important band appears at 1605 cm⁻¹, representing the vibration mode of the C=C bonds. The second band appears at 1321 and 1331 cm⁻¹ attributed to the stretching mode of the pyrrolic ring and the third important band appears at 1040–1054 cm⁻¹, determined by the plane deformation of the C–H bond.

For PPY, ATR FTIR spectra identified the functions: the peak at 780 cm⁻¹ is attributed to C–H out of plane of polypyrrole ring, the peak to 1040 cm⁻¹ represents N–H in plane deformation, the peak located at 1186 cm⁻¹ is assigned to C–N stretching vibration. Ag NP's introduction into the PPY structure leads to some PPY FTIR characteristic bands' displacements, indicating specific interactions between Ag NPs and the PPY functional groups, especially those in the N–H group region.

The SEM images show a classic polypyrrole structure consisting of globular units with average dimensions around 400 nm formed by the collision of smaller globular formations with average dimensions around 200 nm. In the cases of 10%Ag/PPY and 20%Ag/PPY hybrid nanocomposites the PPY covers the silver nanoparticles, as in the core-shell structure.

In making the bioimpedance electrodes, the polypyrrole and Ag/polypyrrole hybrid nanocomposite powders were pressed in disk format. A layer of conductive silver paste on one side of the obtained disks was deposited. Each of the disks thus obtained are arranged on another silver disk of the same diameter. For obtaining the dry polarizable electric bioimpedance sensor, two electrodes arranged at 6 cm from each other were used. The electrical connection is making from the opposite side of each silver disk.

The values obtained for the impedance of the electrode, for all the polymeric materials used, were much lower and almost constant in relation to the total bioimpedance (impedance measured for skin bioimpedance in series with two electrodes impedance), for the whole spectrum of frequencies. For this reason, the conclusions regarding the total bioimpedance can be considered true also for the skin bioimpedance in the first approximation.

The skin electric bioimpedance measurements were performed at two points, by using the dry polarizable electric bioimpedance sensor made of two bioimpedance electrodes, glued on an adhesive strip, and applying a sinusoidal voltage of $2 V_{\text{peak-peak}}$, in the frequency range of 1–300 kHz, at room temperature. The electric bioimpedance measurements were performed on six human subjects, both men and women, between 32 and 59 years old. For all cases, the bioimpedance decreased with frequency, more pronounced in the case of males. At the low frequency of 1 kHz, the bioimpedance values ranged between 16–65.7 k Ω for male subjects and 58.7–155 k Ω for female subjects.

The measurement of the useful signal can be influenced by noise. In the case of measurements of the useful signal in order to obtain total electric bioimpedance by using a precision LCR meter, AGILENT E4980 A type, the measuring probe TL09A ensured an accuracy of 1%. However, to develop ECG equipment that uses the dry polarizable electric bioimpedance sensors made with sensitive materials 10%Ag/PPY or 20%Ag/PPY hybrid nanocomposite it was necessary for the useful signal to be taken in differential mode and the input impedance to be of M Ω values. The problem of shielding and filtering the signal by using bandpass filters must also be solved.

Both AgNPs/PPY hybrid nanocomposites presented a tendency to decrease the measured skin bioimpedance with frequency, but compared to the behaviour of PPY, the bioimpedance values were higher due to the obstruction of the polymer electron gaps by Ag NPs. For hybrid nanocomposites 10%Ag/PPY and 20%Ag/PPY the results obtained indicate the best tendency of quasi-linear decrease of the electric skin bioimpedance with frequency compared to the PPY material.

For the nanocomposite 20%Ag/PPY, the tendency of decreasing the electric skin bioimpedance with frequency was observed but compared to the behaviour of PPY and 10%Ag/PPY the electric skin bioimpedance values were higher, because a higher quantity of Ag NPs inserted in polymer obstructs the hopping of electrons in polymer.

The importance of measurements for skin bioimpedance is given by the possibility of performing studies related to monitoring wound healing in post-operative phases.

The results obtained indicate that both sensitive materials the hybrid nanocomposite 10%Ag/PPY and 20%Ag/PPY can be considered for obtaining the bioimpedance sensors.

Future developments will study the possibility of using the dry polarizable electric bioimpedance sensors at frequencies lower than 100 Hz as well as higher than 300 kHz, in order to take over the signals of the ECG (electrocardiogram), EMG (electromyogram) and EEG (electroencephalography) types. These studies and further developments will be performed for a larger number of subjects and will involve statistical data processing.

Author Contributions: G.T. performed the synthesis of the polypyrrole (PPY), made three types of dry polarizable electric bioimpedance sensors and provided the first draft of the paper while the other authors contributed technical input in their areas of specialty. L.P.-D. performed the conceptualization and investigation activities, provided the guidance for the analysis and the design of the experiments, performed the experiments, analyzed the data and supported the design of the three types of dry polarizable electric bioimpedance sensors. E.-M.L. performed the RAMAN spectrometry, the FTIR spectroscopy and provided the present draft of the paper. These first three

authors have an equal contribution and are considered the principal authors. I.I. performed the synthesis of the sensitive material 10%Ag/PPY and 20%Ag/PPY hybrid nanocomposites. V.M. performed the SEM microscopy and elemental analysis EDX. All authors have read and agreed to the published version of the manuscript.

Funding: This research was funded by the Romanian Ministry of Education and Research grant number 46N/2019, PN19310301 and The APC was funded by the authors of the paper.

Institutional Review Board Statement: This study did not require ethical approval.

Informed Consent Statement: Informed consent was obtained from all subjects involved in the study.

Acknowledgments: This work was financially supported by the Romanian Ministry of Education and Research, Program NUCLEU, Contract 46N/2019, PN19310301, “Complex Bioimpedance Measurement System as Support for Vital Function Monitoring and Development of Cardiovascular Impedance Clinical Techniques”, signed with National R&D Institute for Electrical Engineering ICPE-CA.

Conflicts of Interest: The authors declare no conflict of interest.

References

1. Fraczek, M.; Krecicki, T.; Moron, Z.; Krzywaznia, A.; Ociepka, J.; Rucki, Z.; Szczepanik, Z. Measurements of electrical impedance of biomedical objects. *Acta Bioeng. Biomech.* **2016**, *18*, 11–17. [CrossRef]
2. Naranjo-Hernandez, D.; Reina-Tosina, J.; Min, M. Fundamentals, Recent Advances, and Future Challenges in Bioimpedance Devices for Healthcare Applications. *J. Sens.* **2019**, *2019*, 9210258. [CrossRef]
3. Ferrari, L.M.; Sudha, S.; Tarantino, S.; Esposti, R.; Bolzoni, F.; Cavallari, P.; Cipriani, C.; Mattoli, V.; Greco, F. Ultraconformable Temporary Tattoo Electrodes for Electrophysiology. *Adv. Sci.* **2018**, *5*, 1700771. [CrossRef] [PubMed]
4. Takeshita, T.; Yoshida, M.; Takei, Y.; Ouchi, A.; Hinoki, A.; Uchida, H.; Kobayashi, T. Relationship between Contact Pressure and Motion Artifacts in ECG Measurement with Electrostatic Flocked Electrodes Fabricated on Textile. *Sci. Rep.* **2019**, *9*, 5897–5907. [CrossRef] [PubMed]
5. Chen, Y.H.; Op de Beeck, M.; Vanderheyden, L.; Carrette, E.; Mihajlovic, V.; Vanstreels, K.; Grundlehner, B.; Gadeyne, S.; Boon, P.; Van Hoof, C. Soft, Comfortable Polymer Dry Electrodes for High Quality ECG and EEG Recording. *Sensors* **2014**, *14*, 23758–23780. [CrossRef]
6. Rai, P.; Oh, S.; Shyamkumar, P.; Ramasamy, M.; Harbaugh, R.E.; Varadan, V.K. Nano-Bio-Textile Sensors with Mobile Wireless Platform for Wearable Health Monitoring of Neurological and Cardiovascular Disorders. *J. Electrochem. Soc.* **2014**, *161*, B3116–B3150. [CrossRef]
7. Hu, D.L.; Cheng, T.K.; Xie, K.; Lam, R.H.W. Microengineered Conductive Elastomeric Electrodes for Long-Term Electrophysiological Measurements with Consistent Impedance under Stretch. *Sensors* **2015**, *15*, 26906–26920. [CrossRef]
8. Jeong, J.W.; Kim, M.K.; Cheng, H.Y.; Yeo, W.H.; Huang, X.; Liu, Y.H.; Zhang, Y.H.; Huang, Y.G.; Rogers, J.A. Capacitive Epidermal Electronics for Electrically Safe, Long-Term Electrophysiological Measurements. *Adv. Healthc. Mater.* **2014**, *3*, 642–648. [CrossRef]
9. Lee, S.; Kruse, J. Biopotential electrode sensors in ECG/EEG/EMG systems. *Analog Devices* **2008**, *200*, 1–2.
10. Taji, B.; Shirmohammadi, S.; Groza, V.; Batkin, I. Impact of Skin-Electrode Interface on Electrocardiogram Measurements Using Conductive Textile Electrodes. *IEEE Trans. Instrum. Meas.* **2014**, *63*, 1412–1422. [CrossRef]
11. Karplus, K. S2014, BME 101L: Applied Circuits Lab 4 Polarising and Non-polarising Electrodes. Available online: <https://users.soe.ucsc.edu/~karplus/bme101/s14/04-electrodes.pdf> (accessed on 15 October 2020).
12. Kumar, R.; Singh, R.; Hui, D.; Feo, L.; Fraternali, F. Graphene as biomedical sensing element: State of art review and potential engineering applications. *Compos. Part B Eng.* **2018**, *134*, 193–206. [CrossRef]
13. Abu-Saude, M.; Morshed, B.I. Characterisation of a Novel Polypyrrole (PPy) Conductive Polymer Coated Patterned Vertical CNT (pvCNT) Dry ECG Electrode. *Chemosensors* **2018**, *6*, 27. [CrossRef]
14. Kim, J.H.; Jang, W.Y.; Kim, S.S.; Son, J.M.; Park, G.C.; Kim, Y.J.; Jeon, G.R. Development of Bioelectric Impedance Measurement System Using Multi-Frequency Applying Method. *J. Sens. Sci. Technol.* **2014**, *23*, 368–376. [CrossRef]
15. Liu, Y.; Wang, H.; Zhao, W.; Zhang, M.; Qin, H.; Xie, Y. Flexible, Stretchable Sensors for Wearable Health Monitoring: Sensing Mechanisms, Materials, Fabrication Strategies and Features. *Sensors* **2018**, *18*, 645. [CrossRef] [PubMed]
16. Albulbul, A. Evaluating Major Electrode Types for Idle Biological Signal Measurements for Modern Medical Technology. *Bioengineering* **2016**, *3*, 20–30. [CrossRef]
17. Telipan, G.; Pislaru-Danescu, L.; Ion, I. New polypyrrole based bio-sensors for Bio-impedance measurement. *Int. J. Med. Health Sci.* **2019**, *8*, 38–47.
18. Wang, S.H.; Xu, J.; Wang, W.C.; Wang, G.J.N.; Rastak, R.; Molina-Lopez, F.; Chung, J.W.; Niu, S.M.; Feig, V.R.; Lopez, J.; et al. Skin electronics from scalable fabrication of an intrinsically stretchable transistor array. *Nature* **2018**, *555*, 83–88. [CrossRef]

19. Chlaihawi, A.A.; Narakathu, B.B.; Emamian, S.; Bazuin, B.J.; Atashbar, M.Z. Development of printed and flexible dry ECG electrodes. *Sens. Bio Sens. Res.* **2018**, *20*, 9–15. [[CrossRef](#)]
20. Jung, H.C.; Moon, J.H.; Baek, D.H.; Lee, J.H.; Choi, Y.Y.; Hong, J.S.; Lee, S.H. CNT/PDMS Composite Flexible Dry Electrodes for Long-Term ECG Monitoring. *IEEE Trans. Bio Med. Eng.* **2012**, *59*, 1472–1479. [[CrossRef](#)] [[PubMed](#)]
21. Baek, J.Y.; An, J.H.; Choi, J.M.; Park, K.S.; Lee, S.H. Flexible polymeric dry electrodes for the long-term monitoring of ECG. *Sens. Actuators A Phys.* **2008**, *143*, 423–429. [[CrossRef](#)]
22. Yussuf, A.; Al-Saleh, M.; Al-Enezi, S.; Abraham, G. Synthesis and Characterization of Conductive Polypyrrole: The Influence of the Oxidants and Monomer on the Electrical, Thermal, and Morphological Properties. *Int. J. Polym. Sci.* **2018**, *2018*. [[CrossRef](#)]
23. Farghaly, A.A.; Collinson, M.M. Mesoporous Hybrid Polypyrrole-Silica Nanocomposite Films with a Strata-Like Structure. *Langmuir* **2016**, *32*, 5925–5936. [[CrossRef](#)]
24. Sowmiya, G.; Anbarasan, P.M.; Velraj, G. Synthesis, Characterisation and Electrical Conductivity Study of Conductive Polypyrrole doped with Nano Tin Composite for Antibacterial Application. *Int. Res. J. Eng. Technol.* **2017**, *4*, 127–131.
25. Shrestha, B.K.; Ahmad, R.; Shrestha, S.; Park, C.H.; Kim, C.S. Globular Shaped Polypyrrole Doped Well-Dispersed Functionalized Multiwall Carbon Nanotubes/Nafion Composite for Enzymatic Glucose Biosensor Application. *Sci. Rep.* **2017**, *7*, 16191. [[CrossRef](#)]
26. Borthakur, L.J.; Sharma, S.; Dolui, S.K. Studies on Ag/Polypyrrole composite deposited on the surface of styrene-methyl acrylate copolymer microparticles and their electrical and electrochemical properties. *J. Mater. Sci. Mater. Electron.* **2011**, *22*, 949–958. [[CrossRef](#)]
27. Karimullah, A.S.; Cumming, D.R.S.; Riehle, M.; Gadegaard, N. Development of a conducting polymer cell impedance sensor. *Sens. Actuators B Chem.* **2013**, *176*, 667–674. [[CrossRef](#)]
28. Takamatsu, S.; Lonjaret, T.; Crisp, D.; Badier, J.M.; Malliaras, G.G.; Ismailova, E. Direct patterning of organic conductors on knitted textiles for long-term electrocardiography. *Sci. Rep.* **2015**, *5*, 15003. [[CrossRef](#)] [[PubMed](#)]
29. Yan, Y.; Li, H.Q.; Zhang, Y.; Kan, J.Q.; Jiang, T.F.; Pang, H.; Zhu, Z.X.; Xue, H.G. Facile Synthesis of Polypyrrole Nanotubes and Their Supercapacitive Application. *Int. J. Electrochem. Sci.* **2017**, *12*, 9320–9334. [[CrossRef](#)]
30. Percec, S.; Howe, L.; Li, J.; Bagshaw, A.; Peacock, S.; Bolas, N.; Brill, D. Pyrrole polymerisation on polyimide surfaces creates conductive nano-domains. *Polymer* **2013**, *54*, 5754–5761. [[CrossRef](#)]
31. George, P.M.; Lyckman, A.W.; LaVan, D.A.; Hegde, A.; Leung, Y.; Avasare, R.; Testa, C.; Alexander, P.M.; Langer, R.; Sur, M. Fabrication and biocompatibility of polypyrrole implants suitable for neural prosthetics. *Biomaterials* **2005**, *26*, 3511–3519. [[CrossRef](#)]
32. Gómez-Quintero, T.; Arroyo-Ornelas, M.A.; López-Marín, L.M.; Castaño-Meneses, V.M.; Garcia-Contreras, R.; Acosta-Torres, L.S.; Arenas-Arrocena, M.C. Cytotoxicity of Polypyrrole and Polyaniline Matrixes for Biosensors. *Acta Sci. Med. Sci.* **2019**, *3*, 81–89.
33. Wang, X.D.; Gu, X.S.; Yuan, C.W.; Chen, S.J.; Zhang, P.Y.; Zhang, T.Y.; Yao, J.; Chen, F.; Chen, G. Evaluation of biocompatibility of polypyrrole in vitro and in vivo. *J. Biomed. Mater. Res. A* **2004**, *68*, 411–422. [[CrossRef](#)] [[PubMed](#)]
34. Fonner, J.M.; Forciniti, L.; Nguyen, H.; Byrne, J.D.; Kou, Y.F.; Syeda-Nawaz, J.; Schmidt, C.E. Biocompatibility implications of polypyrrole synthesis techniques. *Biomed. Mater.* **2008**, *3*, 034124. [[CrossRef](#)] [[PubMed](#)]
35. Ateh, D.D.; Navsaria, H.A.; Vadgama, P. Polypyrrole-based conducting polymers and interactions with biological tissues. *J. R Soc. Interface* **2006**, *3*, 741–752. [[CrossRef](#)]
36. Teran-Jimenez, O.; Rodriguez-Roldan, G.; Hernandez-Rivera, D.; Suaste-Gomez, E. Sensors Based on Conducting Polymers for Measurement of Physiological Parameters. *IEEE Sens. J.* **2017**, *17*, 2492–2497. [[CrossRef](#)]
37. Furno, F.; Morley, K.S.; Wong, B.; Sharp, B.L.; Arnold, P.L.; Howdle, S.M.; Bayston, R.; Brown, P.D.; Winship, P.D.; Reid, H.J. Silver nanoparticles and polymeric medical devices: A new approach to prevention of infection? *J. Antimicrob. Chemother.* **2004**, *54*, 1019–1024. [[CrossRef](#)]
38. Liu, W.Y.; Hu, Y.J.; Hou, Y.L. Ethanol Gas Sensitivity Sensor Based on Roughened POF Taper of Modified Polypyrrole Films. *Sensors* **2020**, *20*, 989. [[CrossRef](#)] [[PubMed](#)]
39. Arjomandi, J.; Shah, A.U.; Bilal, S.; Van Hoang, H.; Holze, R. In situ Raman and UV-vis spectroscopic studies of polypyrrole and poly(pyrrole-2,6-dimethyl-beta-cyclodextrin). *Spectrochim. Acta A Mol. Biomol. Spectrosc.* **2011**, *78*, 1–6. [[CrossRef](#)]
40. Eisazadeh, H. Studying the Characteristics of Polypyrrole and its Composites. *World J. Chem.* **2007**, *2*, 67–74.
41. Fu, Y.Z.; Su, Y.S.; Manthiram, A. Sulfur-Polypyrrole Composite Cathodes for Lithium-Sulfur Batteries. *J. Electrochem. Soc.* **2012**, *159*, A1420–A1424. [[CrossRef](#)]
42. Yin, F.X.; Liu, X.Y.; Zhang, Y.G.; Zhao, Y.; Menbayeva, A.; Bakenov, Z.; Wang, X. Well-dispersed sulfur anchored on interconnected polypyrrole nanofiber network as high performance cathode for lithium-sulfur batteries. *Solid State Sci.* **2017**, *66*, 44–49. [[CrossRef](#)]
43. Nerkar, D.; Panse, S.; Patil, S.; Jaware, S.; Padhye, G. Polypyrrole-silver Nanocomposite: Synthesis and Characterisation. *Sens. Transducers* **2016**, *202*, 76–82.
44. Lungulescu, E.M.; Lingvay, I.; Ungureanu, L.C.; Rus, T.; Bors, A.M. Thermooxidative Behavior of Some Paint Materials in Natural Ester Based Electro-insulating Fluid. *Mater. Plast.* **2018**, *55*, 201–206. [[CrossRef](#)]
45. Lungulescu, E.M.; Sbarcea, G.; Setnescu, R.; Nicula, N.; Ducu, R.; Lupu, A.M.; Ion, I.; Marinescu, V. Gamma Radiation Synthesis of Colloidal Silver Nanoparticles. *Rev. Chim.* **2019**, *70*, 2826–2830. [[CrossRef](#)]
46. Wang, L.F.; Liu, J.Q.; Yang, B.; Yang, C.S. PDMS-Based Low Cost Flexible Dry Electrode for Long-Term EEG Measurement. *IEEE Sens. J.* **2012**, *12*, 2898–2904. [[CrossRef](#)]